β-glucan, a dectin-1 ligand, promotes macrophage M1 polarization via NF-κB/autophagy pathway

XIUYING LI[1*], HONGLI LUO[1*], YUN YE[1], XUAN CHEN[2], YUHONG ZOU[1], JIE DUAN[1] and DONG XIANG[1]

Departments of [1]Pharmacy and [2]Gastrointestinal Surgery,
Affiliated Hospital of Southwest Medical University, Luzhou, Sichuan 646000, P.R. China

Received July 13, 2018; Accepted October 19, 2018

DOI: 10.3892/ijo.2018.4630

Abstract. Pro-inflammatory (M1) macrophages have key roles in atherogenesis. As β-glucan has been demonstrated to exert pro-inflammatory effects, the present study examined whether β-glucan exerts atherogenic effects via converting macrophages into M1 phenotype. The results from reverse transcription-quantitative polymerase chain reaction, flow cytometry, western blotting and transmission electron microscope indicated that M1 macrophage markers inducible nitric oxide synthase and cluster of differentiation 80 were upregulated, dectin-1 (a receptor for β-glucan) expression and nuclear factor (NF)-κB nuclear translocation were promoted, and autophagy level was inhibited following β-glucan treatment of macrophages. Additionally, dectin-1 small interfering RNA (siRNA), autophagy inducer rapamycin and NF-κB inhibitor SN50 reversed the effects of β-glucan on autophagy level and macrophage M1 polarization, suggesting that dectin-1 and NF-κB are upstream of autophagy in β-glucan-induced macrophage M1 polarization. Notably, simultaneous treatment with dectin-1 siRNA and SN50 exhibited similar effects on β-glucan-reduced autophagy compared with dectin-1 siRNA treatment alone. These findings demonstrate that dectin-1 may mediate β-glucan-reduced autophagy through NF-κB in macrophages. Accordingly, results from hematoxylin and eosin staining, western blotting and immunofluorescence staining demonstrated that β-glucan accelerated the progress of atherosclerosis in apolipoprotein E-deficient mice and modulated expression of dectin-1, beclin-1 and light chain 3II/I in aortas similarly to that observed in macrophages. These results indicate that dectin-1 activation by β-glucan exerts atherogenic effects via converting macrophages into M1 phenotype in an NF-κB-autophagy-dependent pathway.

Correspondence to: Dr Xiuying Li, Department of Pharmacy, Affiliated Hospital of Southwest Medical University, 25 Taiping Street, Luzhou, Sichuan 646000, P.R. China
E-mail: lxy421421@163.com

[*]Contributed equally

Abbreviations: NF-κB, nuclear factor-κB; siRNA, small interfering RNA; TEM, transmission electron microscopy; ApoE$^{-/-}$, apolipoprotein E-deficient

Key words: β-glucan, dectin-1, autophagy, macrophage M1 polarization, nuclear factor-κB

Introduction

Macrophages have critical roles in the initiation and progression of atherosclerosis (1), and can be categorized into the M1(classically activated macrophages)/M2(alternatively activated macrophages) phenotype in response to various stimuli in the local microenvironment (2). Polarization of M1 macrophages results in progression and enlargement of an atherosclerotic plaque (3,4). The reversal to M2 macrophages has an anti-atherogenic effect via inflammation resolution, efferocytosis and tissue repair (5,6). Therefore, M1/M2 ratio is a major determinant of plaque development (7). This suggests that targeting macrophages may provide effective therapy for atherosclerosis.

A growing body of evidence indicates that autophagy, an evolutionarily conserved process, is a critical modulator in the progression of atherosclerosis (8-10). Autophagy marker light chain 3 (LC3) was detected in atherosclerotic plaques by western blotting and immunohistochemistry (11), while double-membrane vesicles resembling autophagosomes were detected in macrophages via transmission electron microscopy (TEM) (12). Notably, deletion of autophagy rendered atherosclerotic lesions of mice to have increased apoptosis, necrotic cores and overall lesion complexity (13). Stimulation of autophagy in macrophages using 3-methyladenine and berberine enhances the breakdown of the intracellular lipids and the delivery of cholesterol esters to lysosomes for cholesterol efflux, resulting in the prevention of foam cell formation and atherosclerotic plaque development (14,15). However, a detailed understanding of the role for autophagy in atherosclerotic macrophages is still lacking (16).

Natural product β-glucans, which are derived from bacteria, plants and fungal cell walls, have been demonstrated to activate the immune system in a number of studies (17-19). β-glucans are polymers of glucose linked by n-glycosidic bonds (20). As the major pattern recognition receptor for β-glucans, dectin-1 is mainly expressed by myeloid cells such as macrophages and dendritic cells (21-23). Dectin-1 binding by fungal β-glucan has been demonstrated to initiate phagocytosis, generation of superoxide by the NADPH oxidase and inflammatory cytokine

production on macrophages (24-27). Furthermore, dectin-1 activation by β-glucan converts immunosuppressive tumor associated macrophages into an M1-like phenotype (28). However, it remains to be investigated whether β-glucan may also promote RAW264.7 macrophages into the M1 phenotype. Additionally, it is unknown whether the polarized role of β-glucan on macrophages has any effect on the progression of atherosclerosis.

Dectin-1 activation by β-glucan has been implicated in enhancing fungicidal activity and unconventional protein secretion in macrophages through autophagy (29,30). With regards to the pivotal role of macrophage autophagy in the pathogenesis of atherosclerosis, the hypothesis that dectin-1 binding by β-glucan converts RAW264.7 macrophages into an M1 phenotype via autophagy and is associated with the process of atherogenesis was explored, using (apolipoprotein E-deficient) ApoE$^{-/-}$ mice as an experimental model.

Materials and methods

Reagents. β-glucan (purity, 98.0%), rapamycin and SN50 were purchased from Sigma-Aldrich; Merck KGaA (Darmstadt, Germany). Mouse anti-β-actin antibody (sc-47778) was from Santa Cruz Biotechnology, Inc. (Dallas, TX, USA). Rabbit anti-LC3II/I (ab51520), anti-beclin-1 (ab207612), anti-dectin-1 (ab140039), anti-histone H3 (ab1791) and anti-nuclear factor (NF)-κB p65 (ab207297) rabbit antibodies were from Abcam (Cambridge, MA, USA). Fluorescein isothiocyanate (FITC) anti-mouse cluster of differentiation (CD)80 (553768) and FITC anti-mouse C-C chemokine receptor type 7 (CCR7; 560682) antibodies were from BD Biosciences (Franklin Lakes, NJ, USA). FITC anti-mouse CD206 antibody (C068C2) was from BioLegend, Inc. (San Diego, CA, USA). Control and dectin-1 small interfering RNA (siRNA) were purchased from Shanghai GenePharma Co., Ltd. (Shanghai, China). Bafilomycin A1 (54645) was obtained from Cell Signaling Technology, Inc. (Danvers, MA, USA).

Cell culture and siRNA transfection. RAW264.7 cells were obtained from the American Type Culture Collection (Manassas, VA, USA), and maintained in Dulbecco's modified Eagle's medium (Sigma-Aldrich; Merck KGaA) supplemented with 10% fetal bovine serum (Thermo Fisher Scientific, Inc., Waltham, MA, USA) at 37˚C under humidified conditions with 5% CO_2. siRNA targeting dectin-1 and control non-targeting siRNA were designed and constructed by Shanghai GeneChem Co., Ltd. (Shanghai, China). Cell transfections were performed with the SuperFect fragment (Qiagen, Inc., Valencia, CA, USA) according to the manufacturer's instructions using dectin-1/control siRNA (100 nM) in a 25 ml flask. Knockdown efficiencies of siRNA were determined by western blotting analysis as described below. The siRNA sequences used were as follows: siDectin-1, 5'-GCUGUUACCUAUUUAGCUU-3'; and siNC, 5'-UUCUCCGAACGUGUCACGUtt-3'.

Cell treatment with bafilomycin A1. RAW264.7 cells were pretreated for 14 h at 37˚C with 10 nM bafilomycin A1 dissolved in dimethyl sulfoxide (DMSO) to inhibit the fusion between autophagosomes and lysosomes, and then treated in the presence of SN50 at 37˚C (10 μg/ml) for an additional 12 h. Total RNA was extracted and then subjected to reverse transcription-quantitative polymerase chain reaction (RT-qPCR) to detect the mRNA expression of inducible nitric oxide synthase (iNOS) and arginase-1 (Arg-1). The final concentration of DMSO in the medium of control groups matched that of treatment groups and did not exceed 0.05%.

Cell treatment with rapamycin. RAW264.7 macrophages were exposed to β-glucan (100 μg/ml) at 37˚C. Following 12 h, the cells were incubated at 37˚C with 1.5 nM rapamycin dissolved in DMSO for another 12 h to activate autophagy. The final concentration of DMSO in the medium of control groups matched that of treatment groups and did not exceed 0.05%. Cells were collected for western blotting, flow cytometry and RT-qPCR.

Cell viability assay with MTT. Macrophages were seeded at density of 7.5×10^4 cells/well in 96-well plates and the cell viability was determined by MTT assay. Following treatment with or without β-glucan (25, 50 or 100 μg/ml) for 12 h at 37˚C, the culture supernatant was removed. The MTT assay performed as previously described (31).

Flow cytometry. Flow cytometry analysis was performed as described in a previous study (4). Briefly, macrophages were washed and then resuspended in wash buffer containing PBS with 0.1% NaN_3. Cells were then incubated in 1% bovine serum albumin (Sigma-Aldrich; Merck KGaA) for 30 min at room temperature to block non-specific antigens. For surface staining, cells were incubated for 30 min at 4˚C with FITC anti-mouse CD80 (1:200) and FITC anti-mouse CD206 (1:400). Following incubation, macrophages were washed with PBS and resuspended in 0.5 ml PBS for detection. For intracellular staining, cells were incubated with IC Fixation Buffer (eBioscience; Thermo Fisher Scientific, Inc., Waltham, MA, USA) for 20 min at room temperature and then permeabilized with permeabilization buffer (eBioscience; Thermo Fisher Scientific, Inc.). FITC anti-mouse CCR7 was diluted in intracellular staining perm wash buffer (1 μg per million cells in 100 μl volume) and incubated with cells for 20 min in the dark at room temperature. After washing with intracellular staining perm wash buffer, intracellularly labeled cells were resuspended in 0.5 ml cell staining buffer and analysed using a BD Biosciences FACS CANTOII flow cytometer (BD Biosciences). The data acquired were analyzed with FlowJo software version 6.0 (Tree Star, Inc., Ashland, OR, USA).

Animals. A total of 20 8-week old male ApoE$^{-/-}$ mice weighing ~25 g from Jackson Laboratory (Bar Harbor, ME, USA)were housed in barrier facilities (temperature, 20-26˚C; humidity, 40-70%) in a 12-h light/dark cycle. All experimental mice were allowed *ad libitum* access to food and water. Animal procedures were approved by the Animal Care and Use Committee of The Affiliated Hospital of Southwest Medical University (Luzhou, China).

Animal experimental protocols. Following being fed a high-fat diet (15.8% fat and 1.25% cholesterol) for 8 weeks, ApoE$^{-/-}$ mice were treated with β-glucan orally (800 μg each) or 100 μl

PBS as control group daily for 12 weeks using an intra-gastric gavage needle (n=10, each group). The dose of β-glucan used in the present study was determined according to a previous report (28). At 4 weeks following treatment with β-glucan or PBS, mice were sacrificed with CO_2 at a flow rate of 8 l/min in cages (Shanghai Yuyan Instruments Co., Ltd., China) that were 50x40x40cm in size. Once breathing had arrested, hearts and aortas were harvested for hematoxylin and eosin (H&E) staining, western blotting and immunofluorescence staining, as detailed previously (31). Five different mice tissue specimens were used for staining studies.

Western blotting. Tissues and cells were lysed with radioimmunoprecipitation assay buffer (Sigma-Aldrich; Merck KGaA) and phenylmethanesulfonyl fluoride. The protein concentration was measured using a bicinchoninic acid protein assay reagent kit. Equal amounts (30 μg/sample) of protein were separated on 15% SDS-PAGE and transferred to polyvinylidene difluoride membranes. Membranes were blocked in 5% non-fat milk in PBST (3.2 mM Na_2HPO_4, 0.5 mM KH_2PO_4, 1.3 mM KCl, 135 mM NaCl, 0.05% Tween-20; pH 7.4) for 1 h at room temperature and then were incubated with anti-LC3II/I 1:1,000), anti-beclin-1 (1:1,000), anti-histone H3 (1:1,000), anti-NF-κB p65 (1:1,000) or anti-β-actin (1:2,000) antibodies overnight at 4˚C. Subsequently, the membranes were washed and incubated with a horseradish peroxidase (HRP)-conjugated secondary antibody (1:3,000; 7074; Cell Signaling Technology, Inc.) for 1 h at room temperature. The proteins were visualized and quantified using an enhanced chemiluminescence method (Pierce; Thermo Fisher Scientific, Inc.) and Quantity One software version 4.6.7. (Bio-Rad Laboratories, Inc., Hercules, CA, USA) Furthermore, the translocation of NF-κB into the nucleus was calculated by the ratio of NF-κB p65 and histone H3 (32)

RT-qPCR. Total RNA from treated macrophages was isolated using TRIzol reagent (Life Technologies; Thermo Fisher Scientific, Inc.). cDNA synthesis was performed using Maxima First Strand cDNA Synthesis KitApplied Biosystems; Thermo Fisher Scientific, Inc.)according to the manufacturer's protocol. qPCR was performed using a SYBR-Green PCR Master Mix kit (Tiangen Biotech Co., Ltd., Beijing, China). Primer sequences were as follows: iNOS, forward 5'-CGAAAC GCTTCACTTCCAA-3' and reverse 5'-TGAGCCTATATT GCTGTGGCT-3'; arginase-1, forward 5'-AACACGGCAGTG GCTTTAACC-3' and reverse 5'-GGTTTTCATGTGGCG CATTC-3' and GAPDH, forward 5'-GCCAAAAGGGTC ATCATCTC-3' and reverse 5'-GTAGAGGCAGGGATGATG TTC-3' qPCR was performed under the following conditions: 3 min at 95˚C for 1 cycle, 10 sec at 95˚C, 30 sec at 60˚C for 39 cycles and 95˚C for 5 sec. Relative changes in gene expression were calculated using the $2^{-\Delta\Delta Cq}$ method (33). Total cDNA abundance between samples was normalized using primers specific to the GAPDH gene.

TEM. Murine macrophage RAW264.7 cells were harvested and transferred into 1.5 ml Eppendorf tubes and centrifuged at 1,806 x g for 15 min at room temperature as previously described (16). Cells were fixed at 4˚C in 2.5% glutaraldehyde and 1% tannic acid in 0.1 M sodium cacodylate buffer (pH 7.4) for 1 h, washed in 0.1 M cacodylate buffer, and then post-fixed with 1% OsO_4 at 4˚C for 1 h in the same buffer. The specimens were embedded in Epon for 12 h at 35˚C. Finally, 50-70 nm sections were stained with uranyl acetate (30 min) and lead citrate (10 min) at room temperature. Images were observed using a JEM-2000EX transmission electron microscope at 60 kV.

Immunofluorescent histochemistry. Following sacrifice, the vascular aorta was collected, fixed in 10% formaldehyde solution overnight at 4˚C and embedded in optimal cutting temperature compound. Serial sections (8-mm thick) were cut in the frozen slicer. The tissue sections were blocked in endogenous peroxidase sealant (Beyotime Institute of Biotechnology, Haimen, China) for 10 min at room temperature and then were incubated with rabbit antibody against dectin-1 (1:1,000) overnight at 4˚C. Following washing three times with PBS, the tissues were incubated with HRP-conjugated anti-rabbit immunoglobulin G (1:1,000; 12-348; Merck KGaA) at 37˚C for 1 h. Finally, the tissues were visualized via confocal microscopy at a magnification of x200.

For CD206 and CD80 staining, the tissues were incubated with FITC-labeled CD80 (1:200) or FITC-labeled CD206 (1:400) at 37˚C for 1 h. The fluorescence pattern was analyzed by confocal fluorescence microscopy at a magnification of x200.

Five different mice tissue specimens were used for staining. Specimens belonging to β-glucan-treated group were used.

Statistical analysis. Data are presented as the mean ± standard error of the mean. Differences between two groups were compared using Student's t-test, and differences among three or four groups were analyzed using one-way analysis of variance followed by Bonferroni's post hoc test. Continuous variables were tested for normal distribution using the Kolmogorov-Smirnov test. $P<0.05$ was considered to indicate a statistically significant difference. All calculations were carried out with SPSS version 15.0 (SPSS, Inc., Chicago, IL, USA) and repeated 3 times.

Results

Viability determination of RAW264.7 cells treated with β-glucan. To obtain an appropriate β-glucan concentration in macrophages, an MTT assay was performed to examine the toxicity of β-glucan on macrophages. The cell viability was unchanged with the treatment of β-glucan (25, 50 and 100 μg/ml) for 12 h (Fig. 1A). Significant cell death was observed at a dose of 200 μg/ml) in RAW264.7 cells (Fig. 1A), in comparison with the control group.

β-glucan promotes RAW264.7 macrophage M1 polarization. To investigate the effects of β-glucan on the polarization of RAW264.7 cells, iNOS levels were detected, which is an M1 macrophage marker, induced by different concentrations of β-glucan. Cells were treated with different concentrations (0, 25, 50, 100 and 200 μg/ml) of β-glucan for 12 h (Fig. 1B). Treatment with 100 μg/ml) β-glucan significantly increased iNOS mRNA levels, in comparison with the control group. However, the level of iNOS was markedly decreased when RAW264.7 cells were pretreated with 200 μg/ml β-glucan

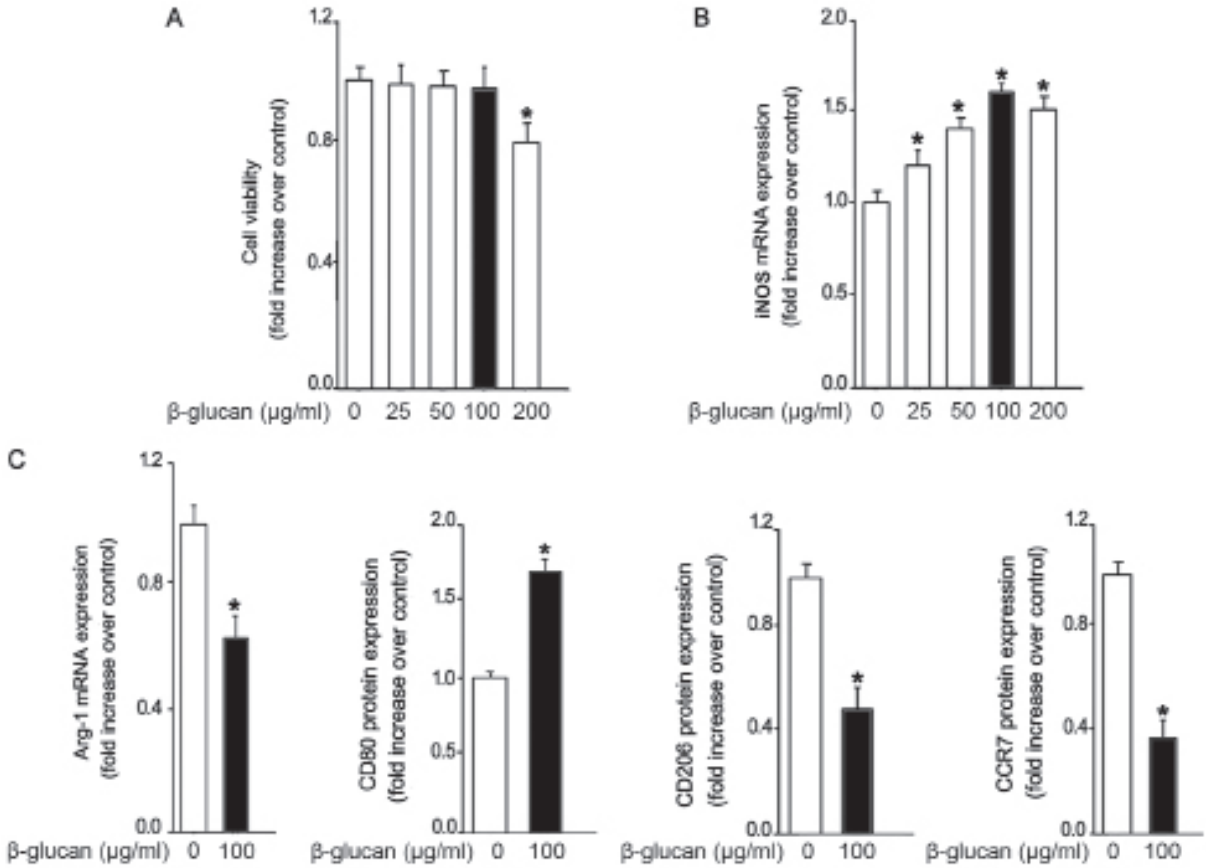

Figure 1. β-glucan promotes macrophages M1 polarization. (A) RAW264.7 cells were cultured for 12 h with or without β-glucan and the cytotoxicity was analyzed by MTT assay. (B and C) Promotion of β-glucan on macrophage M1 polarization. RAW264.7 cells were treated for 12 h with β-glucan. Following treatment, total RNA was extracted and then subjected to reverse transcription-quantitative polymerase chain reaction to detect the mRNA expression of iNOS (M1 macrophage marker) and Arg-1 (M2 macrophage marker). Cells were then collected and CD80 (M1 macrophage marker), CD206 and CCR7 (M2 macrophage markers) were detected by flow cytometry. Data are representative of three independent experiments (mean ± standard error of the mean). *P<0.05 compared with control. iNOS, inducible nitric oxide synthase; Arg-1, arginase-1; CD, cluster of differentiation; CCR7, C-C chemokine receptor type 7.

compared with 100 μg/ml β-glucan, likely as high concentrations of β-glucan result in RAW264.7 cell mortality (34). Therefore, 100 μg/ml β-glucan was chosen for the following experiments. Fig. 1C indicates that M1 macrophage marker CD80 was also upregulated following 100 μg/ml β-glucan treatment, which is consistent with previous findings. Conversely, the M2 markers, such as Arg-1, CD206, CCR7 were reduced following stimulation (Fig. 1C). These data suggest that β-glucan is capable of converting macrophages into an M1-like phenotype and reducing the M2-like phenotype.

Autophagy is associated with β-glucan-induced macrophage M1 polarization. Autophagy is a natural housekeeping mechanism through which superfluous or aged and damaged organelles are removed (35). To explore the association and manner of action of autophagy in the process of β-glucan-induced macrophage M1 polarization, autophagy marker proteins, LC3-II/I and beclin-1 were examined by western blotting following exposure to 100 μg/ml β-glucan for 12 h. The ratio of LC3II/I decreased significantly when compared with the control group (Fig. 2A). The expression levels of beclin-1 were similar to that of LC3-II/I (Fig. 2A). These data suggested that β-glucan may suppress autophagy by downregulating the level of LC3-II/I and beclin-1.

Subsequently, TEM was performed to verify suppressed autophagy in RAW264.7 cells. As demonstrated by the results in Fig. 2B, a markedly decreased number of autophagosome and autolysosome was observed in β-glucan-treated group.

Autophagy in primary human monocytes is induced in the process of cell differentiation (36). However, in the present study, the basal autophagy in RAW264.7 macrophages was suppressed in the process of M1 macrophage polarization. Therefore, it was investigated whether macrophage M1 polarization could be reversed via stimulating autophagy.

To analyze whether autophagy is associated with the polarization of RAW264.7 to M1 macrophages, β-glucan-polarized M1 macrophages were treated with rapamycin and it was demonstrated that rapamycin reversed the inhibitory effects of β-glucan on autophagy in macrophages (Fig. 2C). In comparison with the β-glucan-treated group, a downregulation of iNOS (M1 marker) and an upregulation of Arg1 (M2 marker) was observed at the mRNA level (Fig. 2D), and an obvious increase of CD206 and CCR7 (M2 marker) cells and a significant decrease of CD80 (M1 marker) cells were observed by flow cytometry (Fig. 2E). Meanwhile, rapamycin alone induced beclin-1 and LC3II/I at the protein level, downregulated iNOS (M1 marker) and upregulated Arg1 (M2 marker) at the mRNA level when compared with the control group (Fig. 2F-G). These findings suggest that

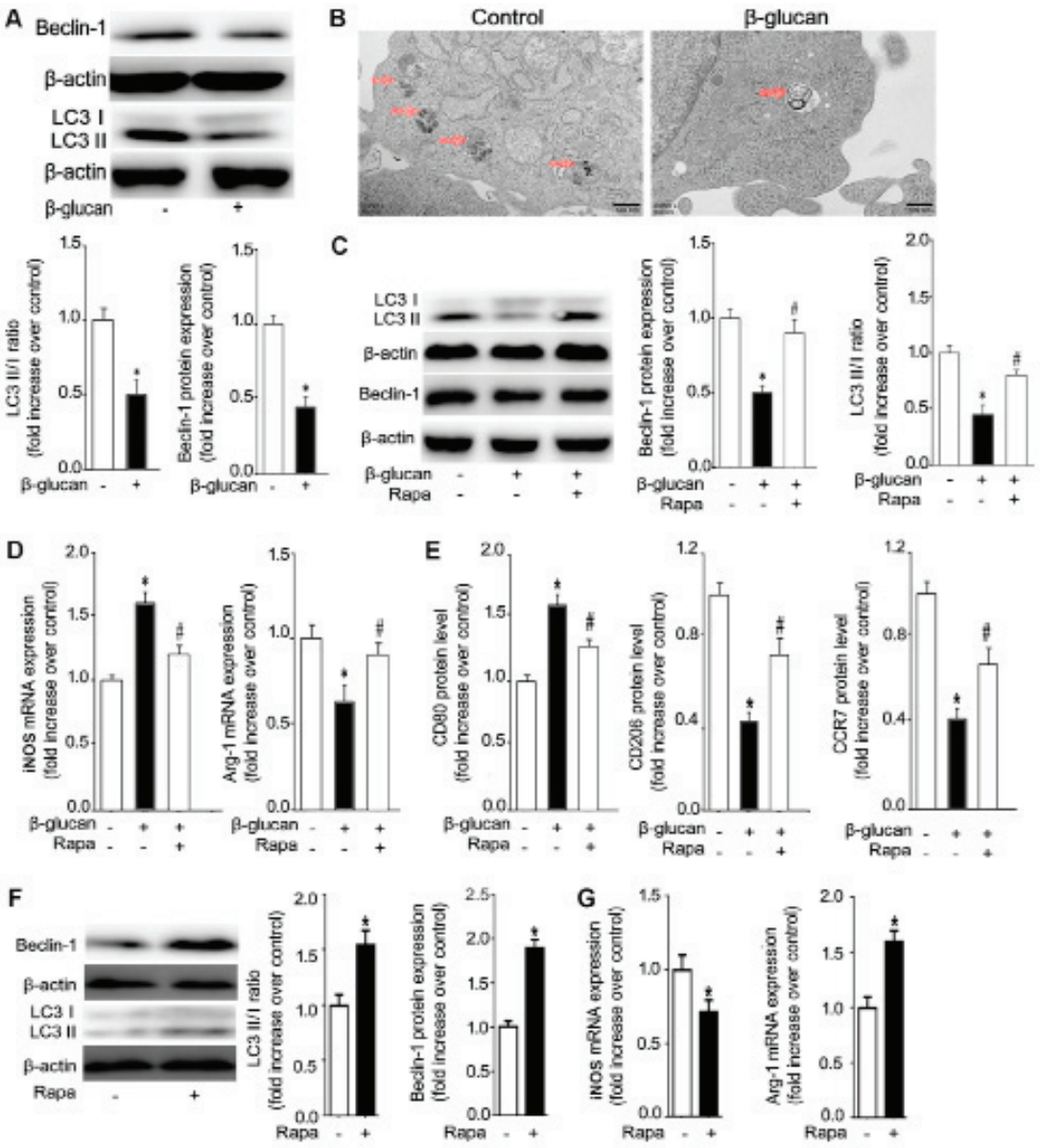

Figure 2. Activation of autophagy reversed β-glucan-induced macrophage M1 polarization. RAW264.7 cells were treated with β-glucan (100 μg/ml) for 12 h, then (A) western blotting was performed to assay the levels of LC3II/I and beclin-1, and (B) electron microscopy was employed to observe numbers of autophagosomes and autolysosomes. Red arrows indicate autophagosomes or autolysosomes. Scale bars=500 nm. RAW264.7 macrophages were exposed to β-glucan (100 μg/ml). Following 12 h, the cells were incubated with 1.5 nM rapamycin for another 12 h. (C) The levels of LC3II/I and beclin-1 were observed by western blotting, or (D) total RNA was extracted and then subjected to RT-qPCR to detect the mRNA expression of iNOS (M1 macrophage marker) and Arg-1 (M2 macrophage marker), or (E) CD80 protein (M1 macrophage marker), CD206 and CCR7 (M2 macrophage markers) were detected by flow cytometry. RAW264.7 macrophages were exposed to 1.5 nM rapamycin for 12 h. (F) The levels of LC3II/I and beclin-1 were observed by western blotting, or (G) total RNA was extracted and then subjected to RT-qPCR to detect the mRNA expression of iNOS and Arg-1. Data are representative of three independent experiments (mean ± standard error of the mean). *P<0.05 compared with control, $^{\#}$P<0.05 compared with β-glucan-treated group. LC3, light chain 3; RT-qPCR, reverse transcription-quantitative polymerase chain reaction; iNOS, inducible nitric oxide synthase; Arg-1, arginase-1; CD, cluster of differentiation; CCR7, C-C chemokine receptor type 7; rapa, rapamycin.

autophagy can reverse the macrophage M1 polarization induced by β-glucan.

Autophagy is regulated by dectin-1 in β-glucan-induced macrophage M1 polarization. Dectin-1 is thought to be the primary receptor for β-glucan (37) and it has been reported that dectin-1 is required for autophagy activation in 60 min and then enhances fungicidal activity in macrophages (29). Therefore, whether dectin-1 is associated with β-glucan-mediated macrophage autophagy and M1 polarization was investigated. RAW264.7 cells were incubated with β-glucan and then subjected to western blotting. β-glucan treatment led to a 1.5-fold increase of dectin-1 protein (Fig. 3A) and a decrease of autophagic activity including lowered level of LC3II/I and beclin-1, and reduction of autophagosome and autolysosome formation in macrophages (Fig. 2A and B). These data suggest that dectin-1 and autophagy are downstream of β-glucan stimulation. To investigate the association between dectin-1 and autophagy in β-glucan-polarized M1 macrophage, a dectin-1-specific siRNA that reduced the dectin-1 protein level by 50% was used (Fig. 3B). Through reducing dectin-1 with siRNA, reduced LC3II/I and beclin-1 protein level and number

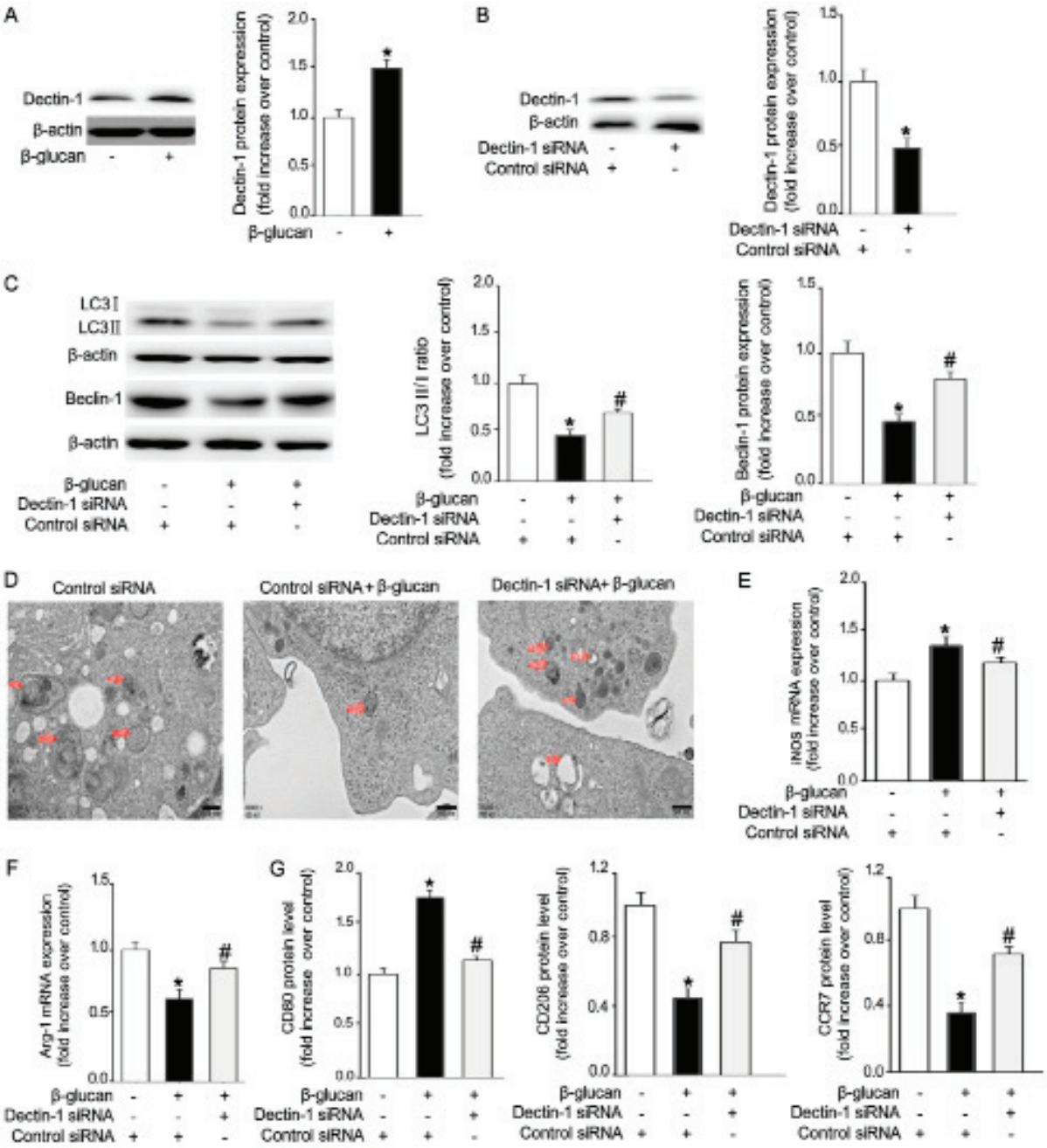

Figure 3. Silencing of dectin-1 reversed β-glucan-induced macrophage M1 polarization. (A) RAW264.7 cells were treated with β-glucan for 12 h, and western blotting was performed to assay the levels of dectin-1. (B) RAW264.7 cells were transfected with dectin-1 siRNA (100 nM) or equal volume of control siRNA for 24 h, and the protein level of dectin-1 was examined by western blotting. RAW264.7 cells were pre-treated with dectin-1 siRNA (100 nM) for 24 h, followed by β-glucan for a further 12 h. (C) The expression of LC3II/I and beclin-1 were observed by western blotting, and (D) numbers of autophagosomes and autolysosomes were observed under electron microscopy. Red arrows indicate autophagosomes or autolysosomes. Scale bars=500 nm. Total RNA was extracted and then subjected to reverse transcription-quantitative polymerase chain reaction to detect the mRNA expression of (E) iNOS (M1 macrophage marker) and (F) Arg-1 (M2 macrophage marker). (G) CD80 (M1 macrophage marker), CD206 and CCR7 (M2 macrophage markers) were detected by flow cytometry. Data are representative of three independent experiments (mean ± standard error of the mean). *P<0.05 compared with control; $^{\#}$P<0.05 compared with (β-glucan+control siRNA)-treated group. siRNA, small interfering RNA; LC3, light chain 3; iNOS, inducible nitric oxide synthase; Arg-1, arginase-1; CD, cluster of differentiation; CCR7, C-C chemokine receptor type 7.

of autolysosome by β-glucan were reversed (Fig. 3C-D), indicating that dectin-1 regulates β-glucan-suppressed autophagy. Furthermore, expression of M1 markers (iNOS and CD80) in RAW264.7 cells with β-glucan were significantly reduced following transfection with dectin-1 siRNA, compared with that in the cells incubated with β-glucan and infected with control siRNA, whereas the opposite results were obtained in M2 markers (Arg-1, CD206, CCR7) detection (Fig. 3E-G). These data indicate that the molecular mechanism of dectin-1-autophagy serves a key role in β-glucan-induced macrophage M1 polarization.

Autophagy is regulated by NF-κB in β-glucan-induced macrophage polarization. NF-κB activities are usually activated during macrophage activation (38). To investigate the effect of β-glucan on translocation of NF-κB into the

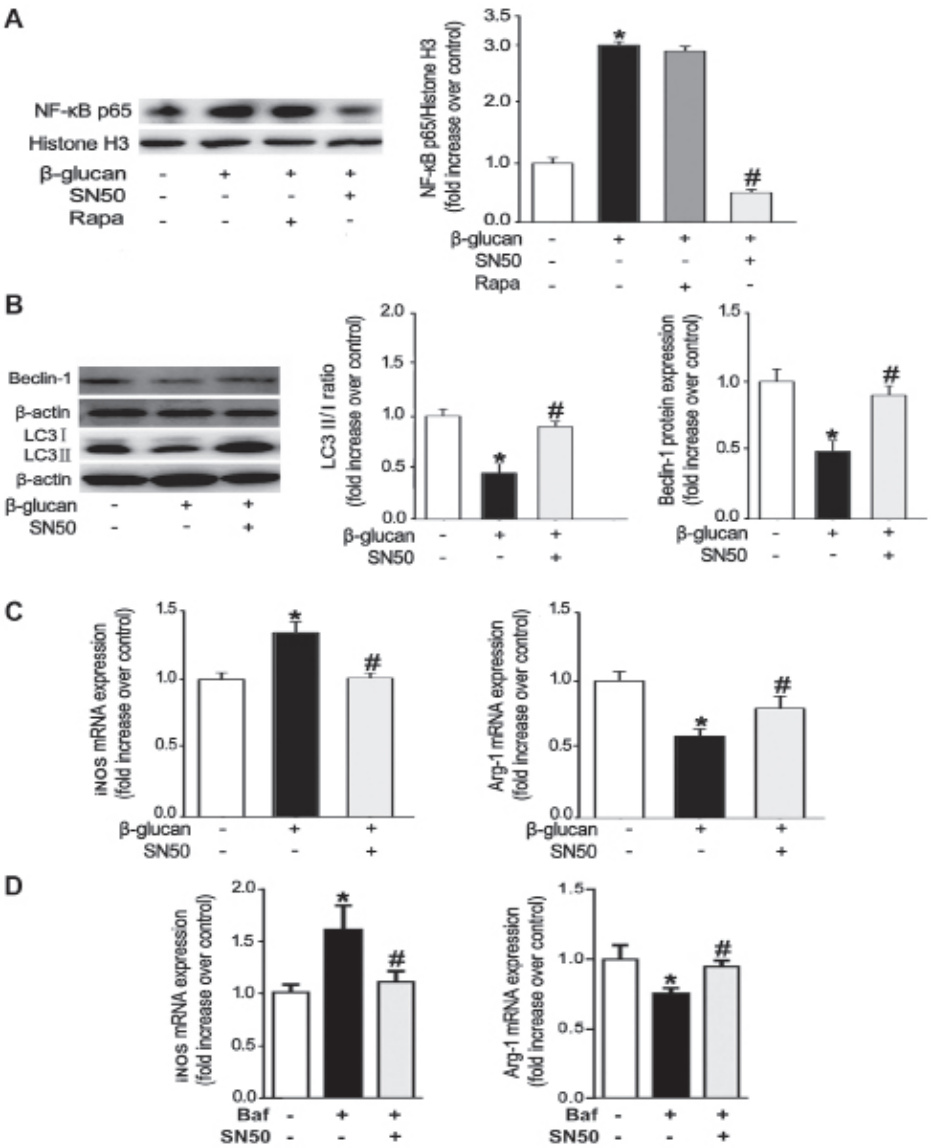

Figure 4. Autophagy is regulated by translocation of NF-κB into the nucleus in β-glucan-induced macrophage M1 polarization. (A) RAW264.7 cells were treated with β-glucan (100 μg/ml) for 12 h, followed by 1.5 nM rapamycin or SN50 for another 12 h. Nuclear extracts were prepared and the protein level of NF-κB p65 was detected by western blotting. RAW264.7 cells were treated with β-glucan (100 μg/ml) for 12 h, and then treated in the presence of SN50 for an additional 12 h. (B) The expression of LC3II/I and beclin-1 were observed by western blotting, or (C) total RNA was extracted and then subjected to RT-qPCR to detect the mRNA expression of iNOS (M1 macrophage marker) and Arg-1 (M2 macrophage marker). RAW264.7 cells were treated with bafilomycin A1 (10 nM) for 14 h, and then treated in the presence of SN50 for an additional 12 h, total RNA was extracted and then subjected to RT-qPCR to detect the mRNA expression of Arg-1 and iNOS (D). Data are representative of three independent experiments (mean ± standard error of the mean). *P<0.05 compared with control, $^{\#}$P<0.05 compared with β-glucan-treated group. NF-κB, nuclear factor-κB; LC3, light chain 3; RT-qPCR, reverse transcription-quantitative polymerase chain reaction; iNOS, inducible nitric oxide synthase; Arg-1, arginase-1; rapa, rapamycin; baf, bafilomycin A1.

nucleus, the nucleoprotein and plasma protein was extracted separately and histone H3 was used as an internal control of nucleoprotein. It was demonstrated that NF-κB p65/histone H3 increased significantly following the treatment of β-glucan when compared with the control group (Fig. 4A).

To examine the association between autophagy and NF-κB in β-glucan-induced macrophages, the expression of autophagy was promoted using rapamycin and NF-κB was blocked by SN50 (the specific inhibitor of NF-κB). As presented above, the expression of autophagic markers LC3II/I and beclin-1 was induced by rapamycin (Fig. 2F), and rapamycin inhibited the M1 polarizaiton of macrophages induced by β-glucan (Fig. 2D and E), however, rapamycin had no significant effect on translocation of NF-κB (Fig. 4A). The specific inhibitor of NF-κB, SN50, has been reported to suppress NF-κB p65/histone H3 and increase the expression of the NF-κB inhibitor IκBα (in the cytoplasm) (39,40). SN50 significantly inhibited β-glucan-induced expression of NF-κBp65/histone H3 (Fig. 4A). Compared with β-glucan-treated group, SN50 significantly increased autophagic markers LC3II/I and beclin-1 (Fig. 4B) in addition to inhibiting β-glucan-induced M1 polarization (Fig. 4C). These data suggest that β-glucan suppressed autophagy via promoting NF-κB nucleus translocation during macrophage M1 polarization. The macrophages were further treated with bafilomycin A1, which inhibits the fusion between autophagosomes and lysosomes, thereby preventing maturation of autophagic vacuoles and degradation of LC3II and p62 (41). Bafilomycin A1 treatment had similar

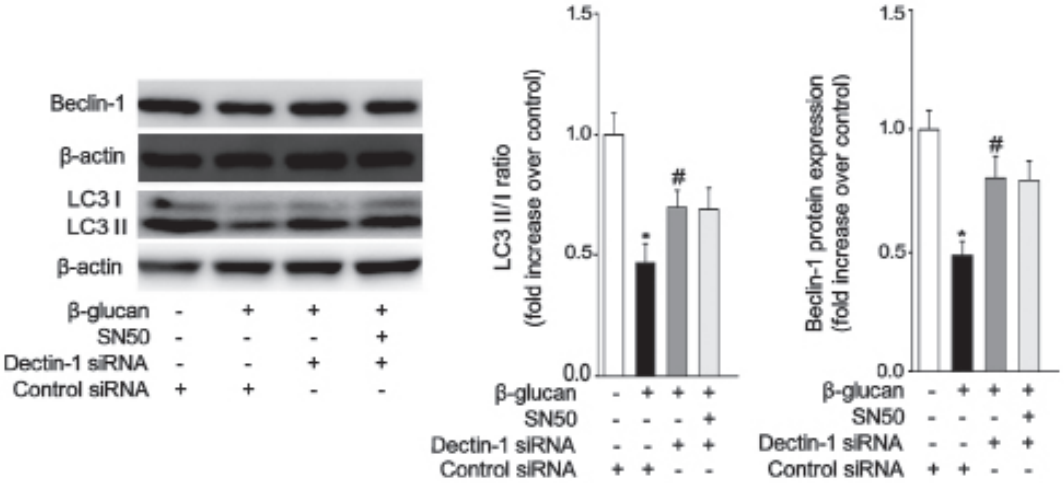

Figure 5. NF-κB inhibitor SN50 could not further increase dectin-1 siRNA-induced autophagy levels in β-glucan-incubated macrophages. RAW264.7 cells were pre-treated with dectin-1 siRNA for 24 h, followed by β-glucan for an additional 12 h, and then treated with SN50 for an additional 12 h. The expression of LC3II/I and beclin-1 were observed by western blotting. Data are representative of three independent experiments (mean ± standard error of the mean). *P<0.05 compared with control siRNA group, #P<0.05 compared with (control siRNA+ β-glucan)-treated group. NF-κB, nuclear factor-κB; siRNA, small interfering RNA; LC3, light chain 3.

effects to β-glucan on M1 marker (iNOS) and M2 marker (Arg-1) in RAW264.7 cells and SN50 reversed its effects (Fig. 4D).

Dectin-1 mediates autophagy in the process of β-glucan-induced macrophage M1 polarization via NF-κB signaling pathway. The above results demonstrated that autophagy was suppressed by dectin-1 ligand, β-glucan and autophagy was also regulated by NF-κB during β-glucan-induced macrophage M1 polarization. Additionally, it was determined whether dectin-1 mediated autophagy in β-glucan-treated macrophages via the NF-κB signaling pathway. Notably, compared with the dectin-1-silenced alone group, beclin-1 and LC3-II/I levels did not exhibit a further increase in β-glucan-incubated macrophages following treatment with dectin-1 siRNA and NF-κB inhibitor SN50 (Fig. 5). These results suggested that the NF-κB signaling pathway is specifically associated with autophagy suppression caused by dectin-1 activation in the process of β-glucan-induced macrophages M1 polarization.

β-glucan increases atherosclerotic lesion formation in ApoE$^{-/-}$ mice. Morphological observations (Fig. 6A and B) indicated that treatment of 16-week-old ApoE$^{-/-}$ mice with β-glucan (800 μg/day) significantly increased the atherosclerostic lesion formation compared with ApoE$^{-/-}$ mice treated with vehicle.

To verify the results obtained in *in vitro* experiments, the expression level of dectin-1, beclin-1 and LC3II/I was examined in aortas of ApoE$^{-/-}$ mice. Compared with the control group, beclin-1 and LC3II/I were downregulated, whereas dectin-1 was upregulated in ApoE$^{-/-}$ mice treated with β-glucan (Fig. 6C). These results are consistent with the findings of *in vitro* experiments. Additionally, double staining of atherosclerotic plaques of ApoE$^{-/-}$ mice (β-glucan-treated group) coronary artery tissue sections demonstrated that dectin-1 was more highly expressed in CD80-positive macrophages (M1 macrophages) than CD206-positive macrophages (M2 macrophages; Fig. 6D). This is consistent with the *in vitro* results that dectin-1 was enhanced in β-glucan-induced M1 macrophage polarization, and dectin-1 knockdown led to the upregulation of CD206 in M1 macrophages induced by β-glucan.

Discussion

Previous studies have indicated that macrophages in the M1 phenotype are more likely to result in an acute atherothrombotic vascular event (42), however, M2 phenotype is mainly associated with tissue repair and displays phagocytic, pro-angiogenic and pro-fibrotic capacities, enhancing plaque stability (43-45). In terms of the key roles of different phenotypes of macrophages in the pathogenesis and development of atherosclerosis, intervention with macrophage polarization represents a potentially effective therapeutic strategy for atherosclerosis (4). In the present study, the data suggested that dectin-1 was highly expressed both in β-glucan-treated RAW264.7 cells *in vitro* and in the arteries in β-glucan-treated ApoE$^{-/-}$ mice. Furthermore, dectin-1 ligand, β-glucan, converted RAW264.7 cells into M1 phenotype *in vitro*. Conversely, dectin-1-specific siRNA reversed the effects of β-glucan on macrophage M1 polarization. Additionally, β-glucan exhibited atherogenic effects in ApoE$^{-/-}$ mice as demonstrated by the presence of more atherosclerotic lesion formation. These findings suggest that dectin-1 activation by β-glucan participated in the pathogenesis of atherosclerosis possibly via promoting macrophage M1 polarization. However, the precise molecular mechanism by which β-glucan promotes atherosclerosis development remains to be investigated.

Autophagy is a cellular degradation process that captures and eliminates intracellular proteins and aged organelles by delivering them to lysosomes, which helps cells to maintain cellular homeostasis (46). Macrophages are largely accumulated in vulnerable plaques and macrophage autophagy undoubtedly serves an essential role in atherosclerosis (47-50). Emerging evidence suggests that macrophage autophagy enhancement exerts a protective role in atherosclerosis (11,51),

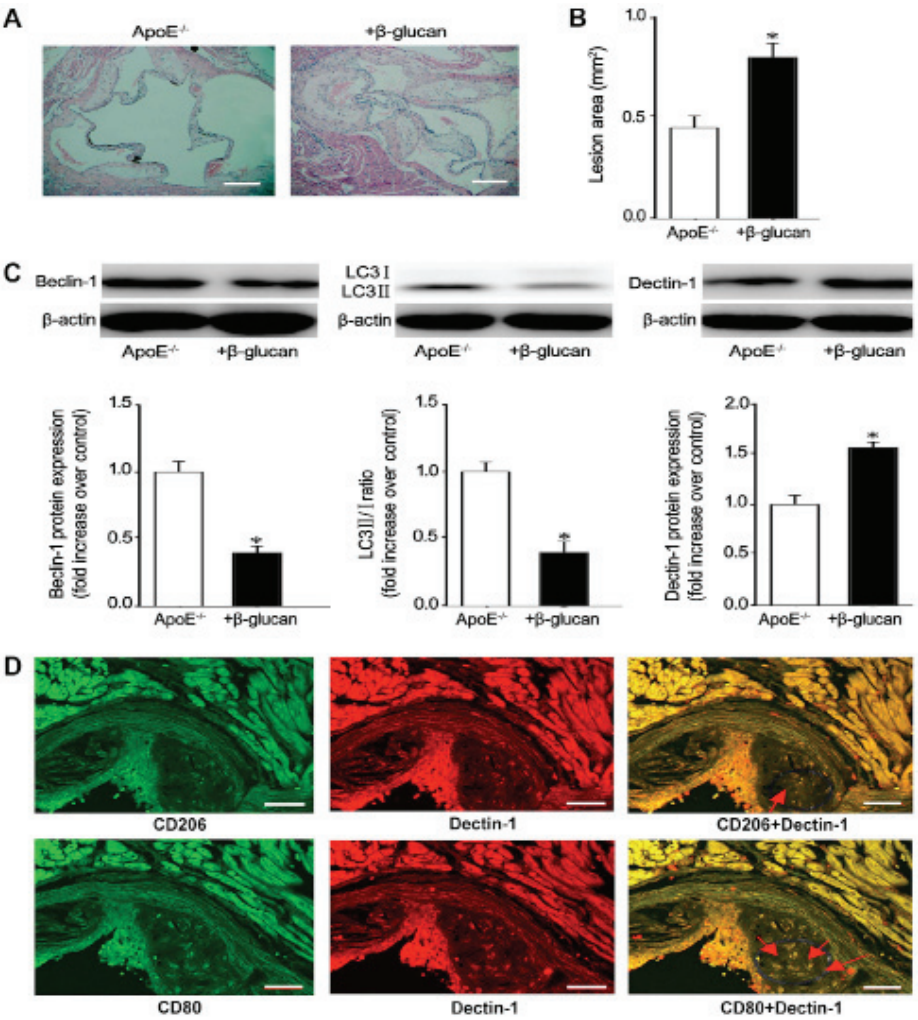

Figure 6. β-glucan promotes atherosclerotic lesion formation in ApoE$^{-/-}$ mice with an increase in the expression of dectin-1 and a decrease in autophagy level. (A) Representative H&E stained aortic sections (magnification, x40; scale bar, 100 μm). (B) Quantification of H&E staining. (C) Following the treatment of ApoE$^{-/-}$ mice, aortas were collected and subjected to western blotting to detect the protein expression of dectin-1, LC3II/I and beclin-1. A representative blot for each is presented. The relative protein levels of dectin-1, LC3II/I and beclin-1 are presented as the mean ± standard error of the mean of the optical density from 3 separate experiments. (D) Double staining of dectin-1 and CD80, or dectin-1 and CD206 in mice coronary atherosclerotic plaque tissue sections in β-glucan-treated group. Typical co-localized staining was indicated with red arrows. Scale bar=10 μm. Figures are representative of staining of five different specimens. *P<0.05 compared with the ApoE$^{-/-}$ mice treated with vehicle. ApoE$^{-/-}$, apolipoprotein E-deficient. H&E, hematoxylin and eosin; LC3, light chain 3; CD, cluster of differentiation.

which has provided a promising therapeutic target to suppress atherosclerosis progression (52). Despite the evidence that macrophage autophagy deficiency leads to increased atherosclerosis, there is little information on the mechanism regarding autophagy inhibition in macrophage M1 polarization during plaque progression. In the present study, it was demonstrated that dectin-1 activation by β-glucan significantly inhibited autophagy as manifested by a decreased hallmark of autophagy-related protein (LC3-II/I and beclin-1) and decreased numbers of autophagosomes and autolysosomes in cultured macrophages. Additionally, the present findings indicated that autophagy agonist rapamycin prevented β-glucan effects on the induction of macrophage M1 polarization, inhibition of beclin-1, LC3-II/I expression, attenuation of macrophage M2 polarization. Rapamycin alone promoted macrophage M2 polarization and inhibited macrophage M1 polarization. Collectively, these data suggest the essential role of autophagy in the β-glucan-mediated induction of macrophage M1 polarization.

C-type lectin receptor dectin-1 has been identified as the main receptor for β-glucan binding and signaling (24). The present findings demonstrated that β-glucan-mediated macrophage M1 conversion is dependent on the dectin-1 receptor. Upon β-glucan stimulation, dectin-1 can recruit LC3 to phagosome and then enhance fungicidal activity in macrophages (29). However, it was demonstrated in the present study that autophagy was downregulated following β-glucan treatment in RAW264.7 cells. This discrepancy may be caused by different experimental conditions (β-glucan incubation time: 60 min vs. 12 h). Similar to autophagy agonist rapamycin, the present findings indicated that gene knockdown of dectin-1 led to upregulated autophagic level in β-glucan-treated RAW264.7 cells, depending on substantially increased expression levels of LC3II/LC3I and beclin-1 protein and the numbers of autophagosome formation. Thus, these results suggested that the dectin-1-autophagy pathway is partially associated with the β-glucan-mediated induction of macrophage M1 conversion. Furthermore, Syk kinase can be directly activated following

dectin-1 stimulation by β-glucan (28). Whether Syk is associated with the β-glucan-induced M1 macrophage formation remains to be elucidated.

NF-κB and autophagy are two major regulators associated with both pathological and physiological processes (53). However, the association between these two signaling pathways still remains unclear in macrophage M1 conversion. SN50 is an NF-κB cell permeable inhibitory peptide, which contains the nuclear localization sequence of the transcription factor NF-κB p50 linked to a peptide cell-permeabilization sequence (39). In addition to inhibiting β-glucan-induced M1 polarization and the expression of NF-κB p65/histone H3, SN50 also increased autophagic marker LC3II/I and beclin-1 inhibited by β-glucan. Meanwhile, SN50 reversed the effects of bafilomycin A1 on the upregulation of M1 marker (iNOS) and downregulation of M2 marker (Arg-1) in RAW264.7 cells. However, the inducer of autophagy rapamycin, which could also decrease β-glucan-induced M1 polarization similar to SN50, had no significant effect on translocation of NF-κB stimulated by β-glucan in RAW264.7 cells. These results suggest that the autophagy of macrophages was regulated by the NF-κB pathways in β-glucan-induced M1 polarization, nevertheless, autophagy exhibited little control over translocation of NF-κB.

In general, the present data indicates that both dectin-1 and NF-κB serve crucial roles in β-glucan-reduced autophagy in macrophage M1 polarization, but the association between dectin-1 and NF-κB in β-glucan-induced macrophages M1 conversion remains unknown. In the present study, it was clearly demonstrated that similar autophagic levels were present in β-glucan-treated RAW264.7 cells prior to dectin-1 silencing plus NF-κB inhibitor as compared with dectin-1 silencing alone. Hence, this suggests that dectin-1-declined autophagy may be dependent on activation of NF-κB signaling pathway in β-glucan-induced macrophage M1 conversion.

In accordance with recent reports from Xu *et al* (20), which demonstrated that β-glucan-induced production of proinflammatory cytokines is critical in the pathogenesis of inflammatory diseases, the present study demonstrated that β-glucan converted macrophages into proinflammatory (M1) phenotype. The findings of β-glucan-invoked promotion of macrophage M1 conversion are not limited to the cell culture system. The present *in vivo* experiments indicated that β-glucan accelerated atherosclerotic progression in $ApoE^{-/-}$ mice. Furthermore, decreased autophagic marker protein LC3II/I and beclin-1, and increased dectin-1 were detected in β-glucan-treated $ApoE^{-/-}$ mice. Meanwhile, a higher dectin-1 level was observed in M1 macrophages compared with M2 macrophages in mice coronary atherosclerotic plaque tissue sections in the β-glucan-treated group. These results are consistent with *in vitro* experiments. The *in vivo* results are contrary to the reports that demonstrated that β-glucan originating from Aureobasidium exerts a favorable effect in decreasing high-fat diet-induced hyperlipemia and associated atherosclerosis on a high-fat diet-induced hyperlipemic hamster model (54). This contradiction may be attributed to differences in animal models.

In conclusion, the present results demonstrated that β-glucan can promote M1 macrophage polarization through increasing dectin-1 receptor, activating NF-κB signaling pathway and then decreasing autophagy. These results indicate that targeting M1 macrophage via reducing dectin-1 can be a potentially effective method for atherosclerosis treatment. The present results not only provide theoretical reasons why β-glucan accelerate atherosclerosis development, but also provide novel targets for clinical treatment.

Acknowledgements

The authors would like to thank Dr Chao Yu (Chongqing Medical University, Chongqing, China) for his experimental assistance. $ApoE^{-/-}$ mice were provided by Dr Xiong Zhong Ruan (Key Laboratory of Lipid and Glucose Metabolism, Chongqing, China).

Funding

The present study was supported by research grants from The National Natural Science Fund (grant no. 81500357), Medical Association of Sichuan Province (grant no. S15040), Affiliated Hospital of Southwest Medical University (grant no. 15044), Southwest Medical University (grant no. 20142D-011) and Beijing Medical Award Foundation (grant no. 16001).

Availability of data and materials

The analyzed data sets generated during the present study are available from the corresponding author on reasonable request.

Authors' contributions

XL and HL designed the experiments; JD and DX performed project administration; YY and XC wrote and edited the manuscript; YZ, HL and YY performed experiments and analyzed the data. All authors have read and approved the final manuscript.

Ethics approval and consent to participate

Animal procedures were approved by the Animal Care and Use Committee of The Affiliated Hospital of Southwest Medical University (Luzhou, China).

Patient consent for publication

Not applicable.

Competing interests

The authors declare that they have no competing interests.

References

1. Fernández-Velasco M, González-Ramos S and Boscá L: Involvement of monocytes/macrophages as key factors in the development and progression of cardiovascular diseases. Biochem J 458: 187-193, 2014.
2. Tabas I and Bornfeldt KE: Macrophage Phenotype and Function in Different Stages of Atherosclerosis. Circ Res 118: 653-667, 2016.

3. Xu R, Li C, Wu Y, Shen L, Ma J, Qian J and Ge J: Role of KCa3.1 Channels in Macrophage Polarization and Its Relevance in Atherosclerotic Plaque Instability. Arterioscler Thromb Vasc Biol 37: 226-236, 2017.
4. Fang S, Xu Y, Zhang Y, Tian J, Li J, Li Z, He Z, Chai R, Liu F, Zhang T, *et al*: Irgm1 promotes M1 but not M2 macrophage polarization in atherosclerosis pathogenesis and development. Atherosclerosis 251: 282-290, 2016.
5. Colin S, Chinetti-Gbaguidi G and Staels B: Macrophage phenotypes in atherosclerosis. Immunol Rev 262: 153-166, 2014.
6. McAlpine CS, Huang A, Emdin A, Banko NS, Beriault DR, Shi Y and Werstuck GH: Deletion of myeloid GSK3α attenuates atherosclerosis and promotes an M2 macrophage phenotype. Arterioscler Thromb Vasc Biol 35: 1113-1122, 2015.
7. Peled M and Fisher EA: Dynamic aspects of macrophage polarization during atherosclerosis progression and regression. Front Immunol 5: 579, 2014.
8. Sergin I, Evans TD, Zhang X, Bhattacharya S, Stokes CJ, Song E, Ali S, Dehestani B, Holloway KB, Micevych PS, *et al*: Exploiting macrophage autophagy-lysosomal biogenesis as a therapy for atherosclerosis. Nat Commun 8: 15750, 2017.
9. Masuyama A, Mita T, Azuma K, Osonoi Y, Nakajima K, Goto H, Nishida Y, Miyatsuka T, Mitsumata M and Watada H: Defective autophagy in vascular smooth muscle cells enhances atherosclerotic plaque instability. Biochem Biophys Res Commun: Oct 11, 2018 (Epub ahead of print).
10. Wang C, Xu W, Liang M, Huang D and Huang K: CTRP13 inhibits atherosclerosis via autophagy-lysosome-dependent degradation of CD36. FASEB J: Sep 17, 2018 (Epub ahead of print).
11. Liao X, Sluimer JC, Wang Y, Subramanian M, Brown K, Pattison JS, Robbins J, Martinez J and Tabas I: Macrophage autophagy plays a protective role in advanced atherosclerosis. Cell Metab 15: 545-553, 2012.
12. Dai S, Wang B, Li W, Wang L, Song X, Guo C, Li Y, Liu F, Zhu F, Wang Q, *et al*: Systemic application of 3-methyladenine markedly inhibited atherosclerotic lesion in ApoE-/- mice by modulating autophagy, foam cell formation and immune-negative molecules. Cell Death Dis 7: e2498, 2016.
13. Kou JY, Li Y, Zhong ZY, Jiang YQ, Li XS, Han XB, Liu ZN, Tian Y and Yang LM: Berberine-sonodynamic therapy induces autophagy and lipid unloading in macrophage. Cell Death Dis 8: e2558, 2017.
14. Martinet W, De Bie M, Schrijvers DM, De Meyer GR, Herman AG and Kockx MM: 7-ketocholesterol induces protein ubiquitination, myelin figure formation, and light chain 3 processing in vascular smooth muscle cells. Arterioscler Thromb Vasc Biol 24: 2296-2301, 2004.
15. Martinet W and De Meyer GR: Autophagy in atherosclerosis: A cell survival and death phenomenon with therapeutic potential. Circ Res 104: 304-317, 2009.
16. Wang T, Zhang L, Hu J, Duan Y, Zhang M, Lin J, Man W, Pan X, Jiang Z, Zhang G, *et al*: Mst1 participates in the atherosclerosis progression through macrophage autophagy inhibition and macrophage apoptosis enhancement. J Mol Cell Cardiol 98: 108-116, 2016.
17. Chan GC, Chan WK and Sze DM: The effects of beta-glucan on human immune and cancer cells. J Hematol Oncol 2: 25, 2009.
18. Li X, Wang J, Wang W, Liu C, Sun S, Gu J, Wang X, Boraschi D, Huang Y and Qu D: Immunomodulatory activity of a novel, synthetic beta-glucan (β-glu6) in murine macrophages and human peripheral blood mononuclear cells. PLoS One 8: e80399, 2013.
19. Karumuthil-Melethil S, Gudi R, Johnson BM, Perez N and Vasu C: Fungal β-glucan, a Dectin-1 ligand, promotes protection from type 1 diabetes by inducing regulatory innate immune response. J Immunol 193: 3308-3321, 2014.
20. Xu J, Liu D, Yin Q and Guo L: Tetrandrine suppresses β glucan induced macrophage activation via inhibiting NF κB, ERK and STAT3 signaling pathways. Mol Med Rep 13: 5177-5184, 2016.
21. Brown GD and Gordon S: Immune recognition. A new receptor for beta-glucans. Nature 413: 36-37, 2001.
22. Brown GD, Taylor PR, Reid DM, Willment JA, Williams DL, Martinez-Pomares L, Wong SY and Gordon S: Dectin-1 is a major beta-glucan receptor on macrophages. J Exp Med 196: 407-412, 2002.
23. Taylor PR, Tsoni SV, Willment JA, Dennehy KM, Rosas M, Findon H, Haynes K, Steele C, Botto M, Gordon S, *et al*: Dectin-1 is required for beta-glucan recognition and control of fungal infection. Nat Immunol 8: 31-38, 2007.
24. Brown GD, Herre J, Williams DL, Willment JA, Marshall AS and Gordon S: Dectin-1 mediates the biological effects of beta-glucans. J Exp Med 197: 1119-1124, 2003.
25. Steele C, Marrero L, Swain S, Harmsen AG, Zheng M, Brown GD, Gordon S, Shellito JE and Kolls JK: Alveolar macrophage-mediated killing of *Pneumocystis carinii* f. sp. *muris* involves molecular recognition by the Dectin-1 beta-glucan receptor. J Exp Med 198: 1677-1688, 2003.
26. Gantner BN, Simmons RM, Canavera SJ, Akira S and Underhill DM: Collaborative induction of inflammatory responses by dectin-1 and Toll-like receptor 2. J Exp Med 197: 1107-1117, 2003.
27. Goodridge HS, Wolf AJ and Underhill DM: Beta-glucan recognition by the innate immune system. Immunol Rev 230: 38-50, 2009.
28. Liu M, Luo F, Ding C, Albeituni S, Hu X, Ma Y, Cai Y, McNally L, Sanders MA, Jain D, *et al*: Dectin-1 activation by a natural product β-glucan converts immunosuppressive macrophages into an M1-like phenotype. J Immunol 195: 5055-5065, 2015.
29. Tam JM, Mansour MK, Khan NS, Seward M, Puranam S, Tanne A, Sokolovska A, Becker CE, Acharya M, Baird MA, *et al*: Dectin-1-dependent LC3 recruitment to phagosomes enhances fungicidal activity in macrophages. J Infect Dis 210: 1844-1854, 2014.
30. Öhman T, Teirilä L, Lahesmaa-Korpinen AM, Cypryk W, Veckman V, Saijo S, Wolff H, Hautaniemi S, Nyman TA and Matikainen S: Dectin-1 pathway activates robust autophagy-dependent unconventional protein secretion in human macrophages. J Immunol 192: 5952-5962, 2014.
31. Li X, Zhou Y, Yu C, Yang H, Zhang C, Ye Y and Xiao S: Paeonol suppresses lipid accumulation in macrophages via upregulation of the ATP binding cassette transporter A1 and downregulation of the cluster of differentiation 36. Int J Oncol 46: 764-774, 2015.
32. Jang CW, Shibata Y, Starmer J, Yee D and Magnuson T: Histone H3.3 maintains genome integrity during mammalian development. Genes Dev 29: 1377-1392, 2015.
33. Livak KJ and Schmittgen TD: Analysis of relative gene expression data using real-time quantitative PCR and the 2(-Delta Delta C(T)) method. Methods 25: 402-408, 2001.
34. Deng X, Zhang J, Liu Y, Chen L and Yu C: TNF-α regulates the proteolytic degradation of ST6Gal-1 and endothelial cell-cell junctions through upregulating expression of BACE1. Sci Rep 7: 40256, 2017.
35. Wang Y, Li Y, Li H, Song H, Zhai N, Lou L, Wang F, Zhang K, Bao W, Jin X, *et al*: Brucella Dysregulates Monocytes and Inhibits Macrophage Polarization through LC3-Dependent Autophagy. Front Immunol 8: 691, 2017.
36. Zhang Y, Morgan MJ, Chen K, Choksi S and Liu ZG: Induction of autophagy is essential for monocyte-macrophage differentiation. Blood 119: 2895-2905, 2012.
37. Vannucci L, Krizan J, Sima P, Stakheev D, Caja F, Rajsiglova L, Horak V and Saieh M: Immunostimulatory properties and antitumor activities of glucans (Review). Int J Oncol 43: 357-364, 2013.
38. Chang CF, Liao KC and Chen CH: 2-Phenylnaphthalene Derivatives Inhibit Lipopolysaccharide-Induced Pro-Inflammatory Mediators by Downregulating of MAPK/NF-κB Pathways in RAW 264.7 Macrophage Cells. PLoS One 12: e0168945, 2017.
39. Chian CF, Chiang CH, Chuang CH, Liu SL and Tsai CL: SN50, a Cell-Permeable Inhibitor of Nuclear Factor-κB, Attenuates Ventilator-Induced Lung Injury in an Isolated and Perfused Rat Lung Model. Shock 46: 194-201, 2016.
40. Kanarek N and Ben-Neriah Y: Regulation of NF-κB by ubiquitination and degradation of the IκBs. Immunol Rev 246: 77-94, 2012.
41. Hou X, Xiao H, Zhang Y, Zeng X, Huang M, Chen X, Birnbaumer L and Liao Y: Transient receptor potential channel 6 knockdown prevents apoptosis of renal tubular epithelial cells upon oxidative stress via autophagy activation. Cell Death Dis 9: 1015, 2018.
42. Kirbis S, Breskvar UD, Sabovic M, Zupan I and Sinkovic A: Inflammation markers in patients with coronary artery disease - comparison of intracoronary and systemic levels. Wien Klin Wochenschr 122 (Suppl 2): 31-34, 2010.
43. Jetten N, Verbruggen S, Gijbels MJ, Post MJ, De Winther MP and Donners MM: Anti-inflammatory M2, but not pro-inflammatory M1 macrophages promote angiogenesis in vivo. Angiogenesis 17: 109-118, 2014.
44. Lee CG, Homer RJ, Zhu Z, Lanone S, Wang X, Koteliansky V, Shipley JM, Gotwals P, Noble P, Chen Q, *et al*: Interleukin-13 induces tissue fibrosis by selectively stimulating and activating transforming growth factor beta(1). J Exp Med 194: 809-821, 2001.

45. Sierra-Filardi E, Vega MA, Sánchez-Mateos P, Corbí AL and Puig-Kröger A: Heme Oxygenase-1 expression in M-CSF-polarized M2 macrophages contributes to LPS-induced IL-10 release. Immunobiology 215: 788-795, 2010.
46. Harris J: Autophagy and cytokines. Cytokine 56: 140-144, 2011.
47. Moore KJ and Tabas I: Macrophages in the pathogenesis of atherosclerosis. Cell 145: 341-355, 2011.
48. Murray PJ and Wynn TA: Protective and pathogenic functions of macrophage subsets. Nat Rev Immunol 11: 723-737, 2011.
49. Zhang Y and Ren J: Epigenetics and obesity cardiomyopathy: From pathophysiology to prevention and management. Pharmacol Ther 161: 52-66, 2016.
50. Zhang Y, Xu X and Ren J: MTOR overactivation and interrupted autophagy flux in obese hearts: A dicey assembly? Autophagy 9: 939-941, 2013.
51. Razani B, Feng C, Coleman T, Emanuel R, Wen H, Hwang S, Ting JP, Virgin HW, Kastan MB and Semenkovich CF: Autophagy links inflammasomes to atherosclerotic progression. Cell Metab 15: 534-544, 2012.
52. Verheye S, Martinet W, Kockx MM, Knaapen MW, Salu K, Timmermans JP, Ellis JT, Kilpatrick DL and De Meyer GR: Selective clearance of macrophages in atherosclerotic plaques by autophagy. J Am Coll Cardiol 49: 706-715, 2007.
53. Baldwin AS: Regulation of cell death and autophagy by IKK and NF-κB: Critical mechanisms in immune function and cancer. Immunol Rev 246: 327-345, 2012.
54. Lim MK, Ku SK, Choi JS and Kim JW: Effect of polycan, a β-glucan originating from Aureobasidium, on a high-fat diet-induced hyperlipemic hamster model. Exp Ther Med 9: 1369-1378, 2015.